Robotic Assessment of Neuromuscular Characteristics using Musculoskeletal Models: A Pilot Study

V. R. Jayanethhthi[a,*], J. Viloria[b], L. G. Wiedemann[a], C. Jarrett[a], A. J. McDaid[a]

[a] *Department of Mechanical Engineering, The University of Auckland, Auckland, 1010, New Zealand*
[b] *Department of Electrical and Computer Engineering, The University of Auckland, Auckland, 1010, New Zealand*

Abstract

Objective: Non-invasive neuromuscular characterization aims to provide greater insight into the effectiveness of existing and emerging rehabilitation therapies by quantifying neuromuscular characteristics relating to force production, muscle viscoelasticity and voluntary neural activation. In this paper, we propose a novel approach to evaluate neuromuscular characteristics, such as muscle fiber stiffness and viscosity, by combining robotic and HD-sEMG measurements with computational musculoskeletal modeling. This pilot study investigates the efficacy of this approach on a healthy population and provides new insight on potential limitations of conventional musculoskeletal models for this application. Methods: Subject-specific neuromuscular characteristics of the biceps and triceps brachii were evaluated using robot-measured kinetics, kinematics and EMG activity as inputs to a musculoskeletal model. Results: Repeatability experiments in five participants revealed large variability within each subjects evaluated characteristics, with almost all experiencing variation greater than 50% of full scale when repeating the same task. Conclusion: The use of robotics and HD-sEMG, in conjunction with musculoskeletal modeling, to quantify neuromuscular characteristics has been explored. Despite the ability to predict joint kinematics with relatively high accuracy, parameter characterization was incon-

*Corresponding author
Email address: vjay721@aucklanduni.ac.nz (V. R. Jayanethhthi)

sistent i.e. many parameter combinations gave rise to minimal kinematic error. Significance: The proposed technique is a novel approach for in vivo neuromuscular characterization and is a step towards the realization of objective in-home robot-assisted rehabilitation. Importantly, the results have confirmed the technical (robot and HD-sEMG) feasibility while highlighting the need to develop new musculoskeletal models and optimization techniques capable of achieving consistent results across a range of dynamic tasks.

Keywords: Electromyography (EMG), HD-sEMG, musculoskeletal modeling, neuromuscular characterization, robotic rehabilitation

---

1. Introduction

Neurological injuries such as cerebral palsy and stroke are among the leading causes of physical disability in the developed world [1]. The effects of these injuries commonly include impairments such as muscle weakness, increased joint spasticity and reduced joint coordination which lead to functional deficits.

Physical and cognitive rehabilitation is typically undertaken to improve impaired motor function resulting from neurological injury. Current rehabilitative care is goal-orientated, focusing on the assessment of quantifiable time-dependent goals against a set of desired patient-specific outcomes [2]. These treatments are often performed at the functional or impairment level, with little or no ability to accurately assess underlying neuromuscular characteristics.

Neuromuscular characteristics relating to muscle force production, muscle viscoelasticity and voluntary neural activation [3] can be estimated using phenomenological models and may provide insights into the underlying physiological properties of muscle [4]. Characteristics such as muscle fiber stiffness and viscosity, could be used as objective measures to test interventions and track patient progress during therapy [5].

The ability to non-invasively diagnose and track underlying physiological characteristics, in-vivo, may help unveil neural recovery mechanisms and could be used to evaluate existing therapies and develop new individualized rehabilita-

tion treatments [6]. For example, it is assumed that hypertonia in spastic cerebral palsy leads to increased muscle fiber stiffness [7], and the ability to directly quantify changes in fiber stiffness may provide further insight into treatment effectiveness. Treatments that may give rise to structural changes in muscle include physiotherapy, splinting and Botulinum Neurotoxin-A. Previous studies regarding non-invasive diagnosis techniques have been for the knee [8], ankle [5] and wrist joint [9]. These model-based approaches use electromyographic (EMG) activity to infer estimates regarding the underlying physiological properties.

Rehabilitation robotics is an area of growing interest in both research and commercialization. There is an increasing demand for physical rehabilitation and a need to increase accessibility to therapy. The ability to provide patients with in-home physical rehabilitation and automatically monitor their progress is highly sought after [10]. To our knowledge, the use of robotic exoskeletons as a supplementary tool for characterizing muscle properties has yet to be explored. Previous integration of robotic exoskeletons with musculoskeletal modeling has focused on the development of control strategies for rehabilitative training [11, 12, 13].

This paper proposes a novel approach to assess an individuals neuromuscular characteristics through the use of rehabilitative robotic exoskeletons (including HD-sEMG) and computational neuro-musculoskeletal modeling. A neuromusculoskeletal model for the elbow, in combination with an upper arm exoskeleton, has been implemented to evaluate neuromuscular characteristics for the biceps and triceps muscle groups. An overview of the proposed technique is illustrated in Fig. 1.

The aim of this study was to conduct a pilot trial on a healthy population to investigate the efficacy of our technical approach and evaluating neuromuscular characteristics using a Hill-based neuro-musculoskeletal model. The objectives were (1) to validate the ability to obtain subjects neuromuscular characteristics that predict/replicate human dynamics; (2) evaluate the reliability of the subject specific assessment; (3) determine the feasibility of using robotics with

neuromuscular modeling as an assessment tool.

2. Methods

2.1. Robotic Exoskeleton

An upper limb robotic exoskeleton designed for rehabilitation therapy was used for the experiments [14]. The exoskeleton has one active degree-of-freedom (DOF), driven by a series elastic actuator, for flexion/extension at the elbow joint, and two passive DOF to account for pronation/supination of the forearm as well as humeroulnar articulation. Hall effect sensors at the active joint accurately track elbow angle and torque. A robust, low-level sliding-mode controller is implemented to control human-robot interaction torques, allowing the exoskeleton to carry out assistive and resistive rehabilitation exercises.

2.2. EMG Acquisition and Processing

EMG activity was captured using high density surface electromyography, or HD-sEMG. Compared to traditional single channel electrodes, this multi-channel system provides additional redundancy to increase measurement robustness. A recent study has also shown HD-sEMG can improve muscle force estimation accuracy [15].

An ActiveTwo HD-sEMG system (*BioSemi B.V., Amsterdam, Netherlands*) was used to record EMG from the biceps and triceps brachii. In total, 64 channels were recorded, 32 per muscle. A 16-by-2 electrode array was placed on each muscle, with both rows aligned parallel along the muscle fiber direction. The center of the electrode arrays was placed on the biceps brachii and triceps long head according to the well-established recommendations given by [16]. This follows the assumption that the activation in each head is indicative of the activation of the entire muscle [17, 18].

All channels were sampled at 2048 Hz. The raw EMG signal was first band-pass filtered through a fourth-order Butterworth filter with cut-off frequencies at 10 Hz and 512 Hz. A 50 Hz notch filter removed mains noise, followed by a

smoothing RMS filter. Using a monopolar configuration, a composite signal was generated by applying a moving maximum filter across all channels, capturing the true skin potential while accounting for poor electrode-skin contact. This filtered EMG signal was normalized for each muscle group using the maximum recorded peak during maximum voluntary contraction.

2.3. Neuro-musculoskeletal Model

The widely adopted Hill-type model can characterize active and passive properties of muscle fiber during contraction [4, 19]. The parameters of this model are largely based on anatomical and physiological principles and are indicative of physical characteristics such as muscle fiber damping and stiffness. Here, an EMG-driven neuro-musculoskeletal model was developed to estimate muscle forces in the biceps and triceps brachii during elbow flexion and extension. These forces were passed to a forward kinematic joint model to predict joint angle. An optimization routine, with an objective function to reduce the error between predicted and measured joint angle, tunes model parameters to each subject.

The filtered EMG signals are first transformed to muscular activation using the procedure established by Buchanan et al. [20]. A Hill-type muscle model of the elbow joint was adapted from [18] to estimate individual muscle forces using muscle activation as input. This EMG-driven model can estimate both active and passive muscle fiber force production during fiber shortening and lengthening. The phenomenological model comprises of a contractile force unit, passive elastic force and passive viscous force components, all in parallel. The model assumes changes in tendon length are negligible.

An existing upper extremity computational model [21] was used to derive a relationship between normalized muscle fiber lengths and moment arms against the elbow joint angle for the biceps brachii (long and short head) and triceps brachii (long, lateral and medial heads). These were used to relate force to the velocity and fiber length relationships in the Hill model.

2.4. Kinematic Joint Modeling

A kinematic model for the elbow joint was adapted from Pau et al. [18]. The model is capable of simulating joint movement, given a set of muscle forces.

The resulting moment (M_{total}) about the joint, in the sagittal plane (flexion/extension), is given by (1),

$$M_{total} = MA_{bicep}.F_{bicep} - MA_{tricep}.F_{tricep} + M_{viscous} + M_{exo} \tag{1}$$

where MA is the instantaneous muscle fiber moment arm, F is the total muscle force from the summation of individual fibers for each group. M_{exo} is the external torque exerted by the exoskeleton. $M_{viscous}$ is the moment due to passive damping forces exerted by biological tissue and fluid.

$M_{viscous}$ is determined using the following equation [18], where ω is angular velocity at the elbow joint and β is the subject-specific damping coefficient for the elbow.

$$M_{viscous} = -\beta\omega \tag{2}$$

Elbow joint angle, $\theta(n)$, and angular velocity can be predicted using the following discrete time kinematic equations,

$$\theta(n) = \theta(n-1) + \omega(n-1).\Delta t + \frac{M_{total}}{2I}.\Delta t^2 \tag{3}$$

$$\omega(n) = \omega(n-1) + \frac{M_{total}}{I}.\Delta t \tag{4}$$

where Δt is the sampling time and I is the combined moment of inertia of the forearm and hand (obtained using OpenSim [22]).

2.5. Subject-Specific Neuromuscular Characteristics

In this study, the neuromuscular characteristics of interest were derived from subject-specific model parameters, that are based on well-known underlying mechanical and electrophysiological properties of muscle and tissue [4, 20]. A summary of all subject-specific characteristics is listed in Table 1. Boundary constraints were enforced according to existing literature [20, 23].

2.6. Neuromuscular Characterization

To evaluate neuromuscular characteristics, a set of experimental data was recorded for each subject during a range of dynamic exercises. EMG, kinematic and kinetic data were measured using the exoskeleton and HD-sEMG system, after which an optimization algorithm calibrated the subject-specific parameters to the individual. The objective for optimization was to reduce the root mean square (RMS) error between the experimentally measured joint angles and model-predicted joint angles. The process was split into two stages to achieve a global optimum with a reduced time cost. First, a global stochastic genetic algorithm optimization [25] defined a global minimum region in the search space (as defined by the boundary constraints for each parameter), followed by an interior point optimization to find the local minimum within this region [26]. The genetic algorithm was set to a population size of 200 with a maximum generation limit of 1,300. A time limit of four hours was placed. When the genetic algorithm finished, the interior point (local) optimization was implemented to reach the final solution.

2.7. Experimental Procedure

In this pilot trial, a convenience sample of five healthy adult male participants was recruited. The mean age was 24.2±2.9 years, and all participants were right-hand dominant. This sample size was deemed satisfactory because the assessment of neuromuscular characteristics is subject-specific and trends regarding the general population are not inferred.

To test the reliability and efficacy of evaluating neuromuscular characteristics participants were asked to carry out four different tasks while wearing the elbow exoskeleton. The selected tasks require a certain degree of motor control and effort. The following tasks were chosen to simulate varying conditions, e.g. changing velocity and muscle activation, in a controlled environment: *T1)* continuous cyclic trajectory tracking; *T2)* chirp signal trajectory tracking; *T3)* cyclic trajectory tracking with resistive torque; *T4)* maximum voluntary isometric contraction. Each task was repeated 3 times, resulting in 12 trials per

subject.

Prior to beginning the experiment, participants skin was prepared by light abrading with sandpaper, followed by cleansing with acetone. Once the electrodes were in place, participants donned the exoskeleton. Throughout the experiment, five variables of interest were recorded, *i*) timestamps *ii*) elbow angle, *iii*) elbow velocity, *iv*) biceps EMG signal, and *v*) triceps EMG signal. Exoskeleton kinematics were logged on a *LabView myRIO* at a frequency of 1 kHz. The exoskeleton was interfaced to PC via *LabView* to provide the participant with visual feedback (real-time angle information) during each task. HD-sEMG was acquired through the *ActiveTwo* measurement system and interfaced to a PC using the *ActiView* software provided by *BioSemi*. Model implementation, data processing and optimization were all done in *Matlab*.

Maximum voluntary contraction (MVC) for the biceps and triceps brachii was recorded according to [27], with a two minute break enforced between measurements. Participants performed a single static maximum contraction for each muscle group, in separate tests, for 10 seconds. Following a two minute break, participants were asked to relax their arm and the muscle tonus was measured. This reading provides a baseline to offset the EMG dataset.

Task 1: Cyclic Trajectory Tracking. The first task involved cyclic motion of the elbow. The exoskeleton was set to back-drivable mode (i.e. zero interaction between the human and robot) and each participant was asked to perform flexion/extension of the elbow through the full range-of-motion (ROM). Next, participants were asked to move their forearm through 5 flexion-extension cycles at a self-selected velocity and an amplitude that corresponded to 75% of the maximum ROM, the latter chosen to avoid overexertion at limits of motion. This period of motion was recorded and used to derive a self-selected frequency of motion.

The self-selected frequency was used to create a sinusoidal set point, with an amplitude again equal to 75% of ROM. The sinusoid was displayed to the user as a graph on the computer screen, along with their elbow angle. Participants

were asked to track this motion for 5 cycles. The task was repeated three times, each separated by at least 30s rest.

Task 2: Chirp Signal Trajectory Tracking. A sinusoidal chirp signal was created as a set point. The amplitude was chosen to be 75% of the recorded ROM from Task 1 and the frequency ranged from 0 Hz to 1.5 times the self-selected frequency obtained from Task 1. Each chirp signal was programmed to increase to the maximum frequency linearly over a period of 20s. The task was repeated three times, each separated by at least 30s rest.

Task 3: Cyclic Trajectory Tracking with Resistive Torque. The exoskeleton was set to apply a resistive anticlockwise torque of 3 Nm. Participants were asked to follow a cyclic trajectory at the self-selected frequency for 20s, with an amplitude equal to 75% of ROM. The task was repeated three times, each separated by at least one minute rest period.

Task 4: Maximum Isometric Contraction. The final task involved recording participants maximum isometric contraction. Participants were asked to fully contract both their biceps and triceps for 20s, whilst holding a constant angle. Three repetitions were performed, separated by two minute rest periods.

Each participant was seated upright during the experiment and the upper arm (humerus) was positioned vertically. Participants were asked to extend and flex their elbow in the sagittal plane and limit shoulder recruitment. To determine the repeatability of neuromuscular characterization, all tasks were repeated three times with a rest period of at least one minute between each task to minimize muscle fatigue.

The number of cycles achieved during some tasks differed across subjects due to differences in self-selected frequency. To standardize the datasets for optimization, the trial data for Task 2 and Task 3 were trimmed to three full cycles. For isometric contraction tasks, the datasets were trimmed when participants began to fatigue during the trial i.e. they could not hold the same angle

any longer.

The University of Auckland Human Participants Ethics Committee (UAHPEC #010810) approved all experimental procedures, and all subjects gave informed consent before participating.

3. Results

3.1. Validation of Model Prediction

The assessment procedure, from data collection to neuro-musculoskeletal modeling, was validated by evaluating the ability to predict joint kinematics across a range of dynamic and isometric tasks. Fig. 2 illustrates the typical results of the four tasks for one subject. The mean RMS error, for predicted vs. robot-measured joint angle, across all subjects were 9.02°, 10.27°, 7.48°and 0.70°for the cyclic, chirp, resistive and isometric contraction tasks, respectively. Fig. 3 summarizes the RMS error for each task across all subjects. The errors are well within the range of existing literature [17, 18, 28].

3.2. Assessment of Neuromuscular Characteristics

The proposed technique optimized the musculoskeletal model to each subject, for each trial of each task, in order to predict neuromuscular characteristics. The neuromuscular characteristics for Subject A are collated in Fig. 4 as a representative example. An additional optimization was carried out using combined data from all recorded trials for each subject as EMG-driven neuromuscular models are often optimized using data from different movement tasks to avoid overfitting [29, 30]. The result from this optimization was compared against the task-specific optimizations for each subject and is summarized in Table 2.

The individual variability (measured as full-scale variation with respect to each characteristic constraint) of the evaluated neuromuscular characteristics for each subject, across each task is illustrated in Fig. 5. The variation in each task highlights the model's low repeatability with the experiments that were performed. In addition, variation in evaluated characteristics does not obviously

improve with increasing accuracy of the dynamic prediction, suggesting an over-fit model.

The variability across all recorded trials is summarized in Fig. 6. It can be seen that there is a high degree of variability (low repeatability) of the model-predicted neuromuscular characteristics, with almost all, excluding C_t, experiencing more than 50% variation across repeated protocols. It should be noted that trials were conducted in laboratory conditions with controlled tasks, and thus raises serious concerns about how the model would perform in real-world scenarios that are prone to even greater experimental error and noise.

In order to determine the task dependency of the model and optimization, optimized parameters from one task were used to predict the kinematics in the other three tasks. The summary of these between task predictions for each subject are outlined in Table 2. Here, the best trial (lowest RMS error) from each task was used to predict the other tasks. In cases where the best trial could not predict all tasks, the next best was used. The table is populated with the average RMS error from all trials recorded for that task. Because of this, some outliers are present where the within-task result is comparatively worse compared to the overall optimization results (bold in the table); not all within-trial optimizations had a low RMS error thus the average RMS error for that task was skewed.

To summarize, using parameters optimized from one task to predict another task resulted in increased kinematic error. This result supports the notion that optimization is a curve fitting exercise for each specific task (or class of tasks e.g. dynamic vs. isometric) and is not transferable to different tasks. These results add evidence to the conclusion that this approach, with such a phenomenological model, is not capable of providing a global solution to a range of diverse tasks, at least not without a much larger experimental data set to use in the parameter optimization. Without evidence that this approach can accurately predict joint behavior with repeatable parameter identification, the approach cannot feasibly be thought to provide accurate information on the underlying neuromuscular characteristics of a wearer.

4. Discussion

We have proposed a new approach for evaluating neuromuscular characteristics in vivo. The proposed method combined three major areas of rehabilitation research; robotics, electrophysiology and musculoskeletal modeling. To our knowledge, the integration of an exoskeleton, HD-sEMG and neuromusculoskeletal modeling is a first, laying the foundation for further research involving these advanced tools.

The model demonstrated the ability to predict joint kinematics relatively accurately thus validating the assessment and experimental procedure. However, pilot trials have highlighted the poor repeatability of the system when evaluating neuromuscular characteristics. Considering the study was limited to healthy participants, the high output variation has exposed the unreliability of the model. Without larger studies and big data sets to prove its efficacy, this model and optimization routine cannot be used to accurately determine characteristics of patients with neurological injuries.

Despite the unfavorable result, this work has highlighted a new potential technique for non-invasive neuromuscular characterization. The use of neuromusculoskeletal modeling to gain insights into underlying physiological properties in the biceps and triceps brachii was yet to be explored. Typically this modeling approach is focused on predicting joint kinetics or kinematics, however, here we have proposed an inverse approach, working backwards to assess subject-specific properties. Alongside this, we have integrated this modeling technique with a robotic assistive device to demonstrate the potential for a fully self-contained rehabilitation tool; combining diagnosis and physical therapy into a single device without, for example, the need for external motion capture cameras. Unlike existing medical imaging systems, such as MRI and ultrasound, neuromuscular assessment through the proposed approach will enable unskilled/untrained users, i.e. patients, to carry out rehabilitative training at home while their performance is continuously monitored remotely. In addition to monitoring structural changes, this technique also enables tracking of neural

activity in the muscle. It is also important to note that this research provides valuable insight into this combined modeling approach and offers a base for other researchers to advance.

High quality HD-sEMG signals were successfully collected while participants performed tasks wearing the upper arm exoskeleton. The robotic system was comfortable during tasks and provided accurate measurement readings of elbow joint angle and torque. The setup time for each subject took up to 20 minutes, mostly due to skin and electrode preparation required for HD-sEMG. Running the data through the optimization routine to evaluate neuromuscular characteristics took up to 5 hours per trial.

There are aspects of the system hardware that need improving before clinical implementation, i.e., to reduce setup and optimization time. Despite this, this work has proved the concept and technical feasibility of combining robotics with neuro-musculoskeletal modeling techniques to provide a potential tool for clinical assessment.

The full-scale variation plot in Fig. 6 yields insight into the experimental sensitivity of the model parameters. It shows the majority of subject-specific characteristics have low sensitivity, i.e., can vary a great deal without affecting the model prediction, which suggests they are more dependent on the specific experimental trial data as opposed to actual neuromuscular characteristics.

In this study, we specifically utilized a global optimization method to search the entire workspace. If this modeling technique is to be used, the global optimum must be found to justify accurate characterization. As such, these findings are a step forward in understanding new potential limitations of this technique. In particular, we have observed there may be certain states of the model that allow for a local minimum to give accurate model prediction with potentially inaccurate estimates of neuromuscular characteristics.

The offline calibration process is essentially a curve-fitting problem to the lumped-parameter, grey box model. This method has typical modeling trade-off implications, where increasing the number of parameters results in a more accurate model prediction with less accurate parameter estimation [5]. The

findings in this research strongly advocate the need for an alternative modeling approach in order to accurately and repeatedly predict neuromuscular characteristics. White box (physiological) approaches, such Huxley models, could be investigated or, alternatively, the existing model could be simplified by experimentally measuring a number of model parameters; for example, physiological cross sectional area of the muscle, calculated by measuring arm circumference [31], can be used to determine active contractile force gain.

The study focused on subject-specific characterization, and therefore, the analysis is performed on individuals as opposed to between subjects. Five participants were included to reduce any individual effects on the repeatability analysis. Between-subject analysis was deemed meaningless due to the high variation of characterization within the same participant. The analysis was based on three trials per task, with rest periods between trials to reduce the effect of fatigue on the results. During the initial pilot trials, significant variation in neuromuscular characteristics was apparent. It was, therefore, evident that three trials per task would be sufficient to provide insights into the models repeatability.

Neuromuscular characterization is largely based on the Hill-type muscle model. While these models are physiologically derived, they contain major simplifying assumptions. The model parameters in question indirectly infer properties about the underlying muscle based on these physiological and anatomical principles. The omission of more detailed physiological properties may limit the usefulness of the assessment. For example, the non-linear activator factors (A_b/A_t) are dependent on many other factors such as motoneuron health and nerve conduction delay. Omitting these subtleties may impact the overall accuracy of the evaluated neuromuscular characteristics. This is a potential drawback of using conventional Hill-type models for this proposed approach. Increasing the number of physiological parameters is possible, however as discussed earlier, care needs to be taken when adding more parameters to a model that is arguably already overfitted.

The muscle fiber length and moment arm relationships were derived from an

upper extremity model [21]. Motion capture is required to accurately scale this model [22]. As we are focused on providing a system for in home rehabilitation robotics to become accessible, we used the OpenSim model database to obtain an average healthy male adult for scaling to match the participants selected. The focus of the study was to test the repeatability of the system and methods, which is not affected by accurate scaling of the model.

HD-sEMG was utilized to ensure a high quality and robust electrophysiological signal was recorded along the length of the muscle, even in dynamic movements where the muscle moves under the skin. Findings from preliminary trials showed the HD-sEMG redundancy was necessary to achieve robust measurements. The greater number of measurement channels increased redundancy against signal artefacts compared to single channel electrode pairs. High-density EMG can glean more detailed information regarding the underlying electromechanical mechanisms of muscle contraction such as number of motor units, innervation zones [32], and conduction velocities [33]. While using this additional information to improve the accuracy of muscle force estimation was considered out-of-scope for this study, in future research we aim to utilize HD-sEMG to its full potential as well as explore the feasibility of real-time neuromuscular characterization.

5. Conclusion

A novel approach for robotic assessment of neuromuscular characteristics using an EMG-based musculoskeletal modeling technique has been proposed. This pilot study has highlighted the potential for poor repeatability of this approach. Optimization of the system resulted in many neuromuscular parameter combinations capable of producing minimal kinematic error. This research has revealed insights into the efficacy of optimizing many design variables of a Hill-type muscle model and will set the foundation to explore new models that are capable of evaluating, in vivo, the underlying characteristics of muscle.

Acknowledgements

This research was supported in part by the Marsden Fund Council from Government funding, managed by the Royal Society of New Zealand. There was no involvement by the sponsor in the study design; in the collection, analysis and interpretation of data; in the writing of the manuscript; and in the decision to submit the article for publication.

References

[1] D. Hirtz, D. J. Thurman, K. Gwinn-Hardy, M. Mohamed, A. R. Chaudhuri, R. Zalutsky, How common are the "common" neurologic disorders?, Neurology 68 (5) (2007) 326–337. doi:10.1212/01.wnl.0000252807.38124.a3.
URL http://www.neurology.org/cgi/doi/10.1212/01.wnl.0000252807.38124.a3

[2] P. Langhorne, J. Bernhardt, G. Kwakkel, Stroke rehabilitation., Lancet 377 (9778) (2011) 1693–702. doi:10.1016/S0140-6736(11)60325-5.
URL http://www.sciencedirect.com/science/article/pii/S0140673611603255

[3] L. M. Paavolainen, a. T. Nummela, H. K. Rusko, Neuromuscular characteristics and muscle power as determinants of 5-km running performance, Med Sci Sports Exerc 31 (1) (1999) 124–130. doi:10.1097/00005768-199901000-00020.
URL http://www.ncbi.nlm.nih.gov/entrez/query.fcgi?cmd=Retrieve&db=PubMed&dopt=Citation&list_uids=9927020

[4] A. Hill, The heat of shortening and the dynamic constants of muscle, Proceedings of the Royal Society of.
URL http://rspb.royalsocietypublishing.org/content/royprsb/126/843/136.full.pdf

[5] L. Bar-On, K. Desloovere, G. Molenaers, J. Harlaar, T. Kindt, E. Aertbeliën, Identification of the neural component of torque during manually-applied spasticity assessments in children with cerebral palsy, Gait & Posture 40 (3) (2014) 346–351. doi:10.1016/j.gaitpost.2014.04.207.

[6] M. Sartori, D. G. Llyod, D. Farina, Neural Data-Driven Musculoskeletal Modeling for Personalized Neurorehabilitation Technologies, IEEE Transactions on Biomedical Engineering 63 (5) (2016) 879–893. doi:10.1109/TBME.2016.2538296.
URL http://ieeexplore.ieee.org/lpdocs/epic03/wrapper.htm?arnumber=7440844

[7] L. Bar-On, G. Molenaers, E. Aertbeliën, A. Van Campenhout, H. Feys, B. Nuttin, K. Desloovere, K. Desloovere, Spasticity and Its Contribution to Hypertonia in Cerebral Palsy, BioMed Research International 2015 (2015) 1–10. doi:10.1155/2015/317047.
URL http://www.hindawi.com/journals/bmri/2015/317047/

[8] S. Pfeifer, H. Vallery, M. Hardegger, R. Riener, E. J. Perreault, Model-Based Estimation of Knee Stiffness, IEEE Transactions on Biomedical Engineering 59 (9) (2012) 2604–2612. doi:10.1109/TBME.2012.2207895.
URL http://ieeexplore.ieee.org/lpdocs/epic03/wrapper.htm?arnumber=6237517

[9] K. L. de Gooijer-van de Groep, E. de Vlugt, H. J. van der Krogt, . Helgadóttir, J. H. Arendzen, C. G. Meskers, J. H. de Groot, Estimation of tissue stiffness, reflex activity, optimal muscle length and slack length in stroke patients using an electromyography driven antagonistic wrist model, Clinical Biomechanics 35 (2016) 93–101. doi:10.1016/j.clinbiomech.2016.03.012.

[10] R. C. V. Loureiro, W. S. Harwin, K. Nagai, M. Johnson, Advances in upper limb stroke rehabilitation: a technology push, Medical & Biological Engineering & Computing 49 (10) (2011) 1103–1118. doi:10.1007/

s11517-011-0797-0.
URL http://link.springer.com/10.1007/s11517-011-0797-0

[11] Y. Ma, S. Q. Xie, Y. Zhang, A patient-specific biological command based controller for the Human-inspired robotic exoskeleton (HuREx): A case study for gait-swing assistance robot, in: 2014 IEEE International Conference on Mechatronics and Automation, IEEE, 2014, pp. 286–291. doi:10.1109/ICMA.2014.6885710.
URL http://ieeexplore.ieee.org/lpdocs/epic03/wrapper.htm?arnumber=6885710

[12] Y. Ma, S. Xie, Y. Zhang, A patient-specific EMG-driven neuromuscular model for the potential use of human-inspired gait rehabilitation robots, Computers in Biology and Medicine 70 (2016) 88–98. doi:10.1016/j.compbiomed.2016.01.001.

[13] E. Ceseracciu, A. Mantoan, M. Bassa, J. C. Moreno, J. L. Pons, G. A. Prieto, A. J. del Ama, E. Marquez-Sanchez, A. Gil-Agudo, C. Pizzolato, D. G. Lloyd, M. Reggiani, A flexible architecture to enhance wearable robots: Integration of EMG-informed models, in: 2015 IEEE/RSJ International Conference on Intelligent Robots and Systems (IROS), IEEE, 2015, pp. 4368–4374. doi:10.1109/IROS.2015.7353997.
URL http://ieeexplore.ieee.org/document/7353997/

[14] C. Jarrett, A. J. McDaid, Robust control of a cable-driven soft exoskeleton joint for intrinsic human-robot interaction, IEEE Transactions on Neural Systems & Rehabilitation Engineering.

[15] S. Boudaoud, S. Allouch, M. Al Harrach, F. Marin, On the benefits of using HD-sEMG technique for estimating muscle force, Computer methods in biomechanics and biomedical engineering 18 Suppl 1 (2015) 1890–1891. doi:10.1080/10255842.2015.1070578.
URL http://www.tandfonline.com.ezproxy.auckland.ac.nz/doi/full/10.1080/10255842.2015.1070578

[16] H. J. Hermens, B. Freriks, C. Disselhorst-Klug, G. Rau, Development of recommendations for SEMG sensors and sensor placement procedures, Journal of Electromyography and Kinesiology 10 (5) (2000) 361–374. doi:10.1016/S1050-6411(00)00027-4.

[17] T. K. K. Koo, A. F. T. Mak, Feasibility of using EMG driven neuromusculoskeletal model for prediction of dynamic movement of the elbow., Journal of electromyography and kinesiology : official journal of the International Society of Electrophysiological Kinesiology 15 (1) (2005) 12–26. doi:10.1016/j.jelekin.2004.06.007.
URL http://www.ncbi.nlm.nih.gov/pubmed/15642650

[18] J. W. L. Pau, S. S. Q. Xie, A. J. Pullan, Neuromuscular Interfacing: Establishing an EMG-Driven Model for the Human Elbow Joint, IEEE Transactions on Biomedical Engineering 59 (9) (2012) 2586–2593. doi:10.1109/TBME.2012.2206389.
URL http://ieeexplore.ieee.org/lpdocs/epic03/wrapper.htm?arnumber=6226835

[19] J. Winters, Hill-Based Muscle Models: A Systems Engineering Perspective, Multiple Muscle systems (1990) 69–93.
URL http://link.springer.com/chapter/10.1007/978-1-4613-9030-5_5

[20] T. S. Buchanan, D. G. Lloyd, K. Manal, T. F. Besier, Neuromusculoskeletal Modeling: Estimation of Muscle Forces and Joint Moments and Movements from Measurements of Neural Command, Journal of applied biomechanics 20 (4) (2004) 367–95.
URL http://www.pubmedcentral.nih.gov/articlerender.fcgi?artid=1357215&tool=pmcentrez&rendertype=abstract

[21] K. R. Saul, X. Hu, C. M. Goehler, M. E. Vidt, M. Daly, A. Velisar, W. M. Murray, Benchmarking of dynamic simulation predictions in two software platforms using an upper limb musculoskeletal model., Computer methods

in biomechanics and biomedical engineering 18 (13) (2015) 1445–58. doi:10.1080/10255842.2014.916698.
URL http://www.ncbi.nlm.nih.gov/pubmed/24995410

[22] S. L. Delp, F. C. Anderson, A. S. Arnold, P. Loan, A. Habib, C. T. John, E. Guendelman, D. G. Thelen, OpenSim: Open-Source Software to Create and Analyze Dynamic Simulations of Movement, IEEE Transactions on Biomedical Engineering 54 (11) (2007) 1940–1950. doi:10.1109/TBME.2007.901024.
URL http://ieeexplore.ieee.org/document/4352056/

[23] Y. Lee, J. A. Ashton-Miller, Effects of Age, Gender and Level of Co-contraction on Elbow and Shoulder Rotational Stiffness and Damping in the Impulsively End-Loaded Upper Extremity., Annals of biomedical engineering 43 (5) (2015) 1112–22. doi:10.1007/s10439-014-1185-3.
URL http://www.ncbi.nlm.nih.gov/pubmed/25395216

[24] Q. Shao, D. N. Bassett, K. Manal, T. S. Buchanan, An EMG-driven model to estimate muscle forces and joint moments in stroke patients., Computers in biology and medicine 39 (12) (2009) 1083–8. doi:10.1016/j.compbiomed.2009.09.002.
URL http://www.pubmedcentral.nih.gov/articlerender.fcgi?artid=2784179&tool=pmcentrez&rendertype=abstract

[25] A. Conn, N. Gould, P. Toint, A Globally Convergent Augmented Lagrangian Algorithm for Optimization with General Constraints and Simple Bounds, SIAM Journal on Numerical Analysis.
URL http://www.jstor.org/stable/2157828

[26] R. H. Byrd, J. C. Gilbert, J. Nocedal, A trust region method based on interior point techniques for nonlinear programming, Mathematical Programming 89 (1) (2000) 149–185. doi:10.1007/PL00011391.
URL http://link.springer.com/10.1007/PL00011391

[27] P. Konrad, The abc of emg, A practical introduction to kinesiological ... (April) (2005) 1–60. doi:10.1016/j.jacc.2008.05.066.
URL http://demotu.org/aulas/controle/ABCofEMG.pdf

[28] M. Pang, S. Guo, Q. Huang, H. Ishihara, H. Hirata, Electromyography-Based Quantitative Representation Method for Upper-Limb Elbow Joint Angle in Sagittal Plane, Journal of Medical and Biological Engineering 35 (2) (2015) 165–177. doi:10.1007/s40846-015-0033-8.
URL http://link.springer.com/10.1007/s40846-015-0033-8

[29] D. G. Lloyd, T. F. Besier, An EMG-driven musculoskeletal model to estimate muscle forces and knee joint moments in vivo, Journal of Biomechanics 36 (6) (2003) 765–776. doi:10.1016/S0021-9290(03)00010-1.
URL http://www.sciencedirect.com/science/article/pii/S0021929003000101

[30] M. Sartori, M. Reggiani, D. Farina, D. G. Lloyd, EMG-driven forward-dynamic estimation of muscle force and joint moment about multiple degrees of freedom in the human lower extremity., PloS one 7 (12) (2012) e52618. doi:10.1371/journal.pone.0052618.
URL http://journals.plos.org/plosone/article?id=10.1371/journal.pone.0052618

[31] Y.-W. Chang, F.-C. Su, H.-W. Wu, K.-N. An, Optimum length of muscle contraction.
URL http://ac.els-cdn.com/S0268003399000145/1-s2.0-S0268003399000145-main.pdf?_tid=60a6a4f0-2d7a-11e7-8e13-00000aacb35d&acdnat=1493539109_062db35bd5ca3ac2274002fa10aafdf3

[32] R. Merletti, A. Holobar, D. Farina, Analysis of motor units with high-density surface electromyography, Journal of Electromyography and Kinesiology 18 (6) (2008) 879–890. doi:10.1016/j.jelekin.2008.09.002.

[33] A. Holobar, D. Farina, Blind source identification from the multichannel surface electromyogram., Physiological measurement 35 (7) (2014) 143–65. doi:10.1088/0967-3334/35/7/R143.
URL http://www.ncbi.nlm.nih.gov/pubmed/24943407

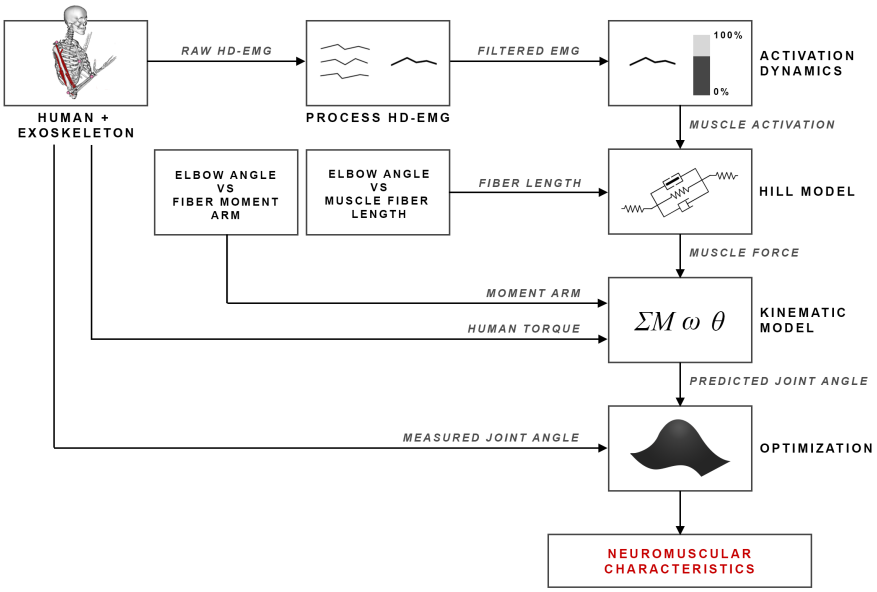

Figure 1: Non-invasive in-vivo neuromuscular characterization using neuro-musculoskeletal modeling techniques.

Table 1: Subject-Specific Neuromuscular Characteristics

Symbol	Subject-Specific Characteristic
R_b, R_t	Active contractile force gain [24, 18]
C_b, C_t	Passive fiber elasticity [18]
B_b, B_t	Passive fiber viscosity [18]
A_b, A_t	Non-linear activation factor [20]
$C1_b$, $C1_t$	Muscle twitch response [20]
$C2_b$, $C2_t$	
β	Passive elbow joint damping [18]

b = biceps brachii, t = triceps brachii

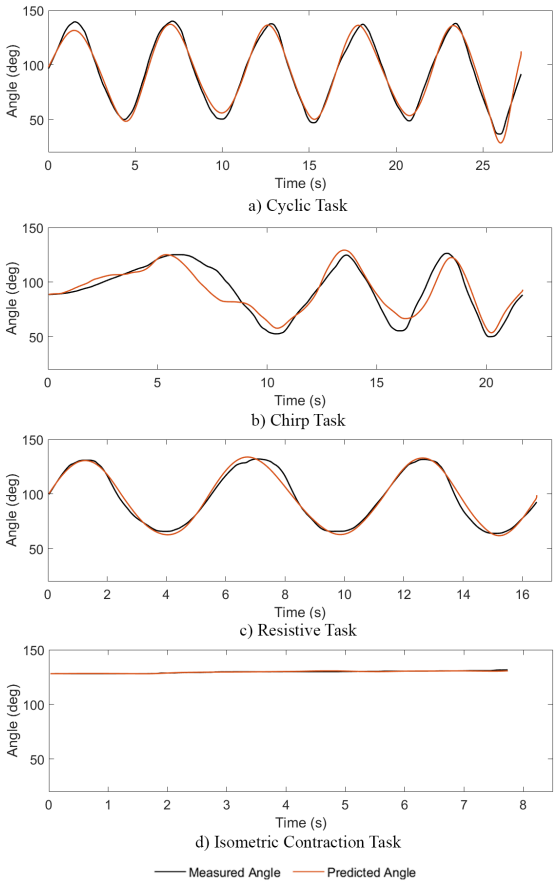

Figure 2: Model predictions for elbow joint angle during a) cyclic b) chirp c) resistive and d) isometric contraction tasks with RMS error of 4.41°, 8.83°, 3.53°and 0.31°, respectively, for Subject A.

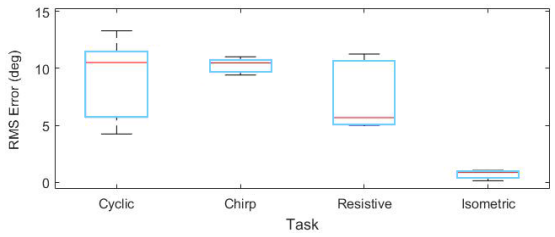

Figure 3: Box plot illustrating the spread of RMS error for each task across all five subjects.

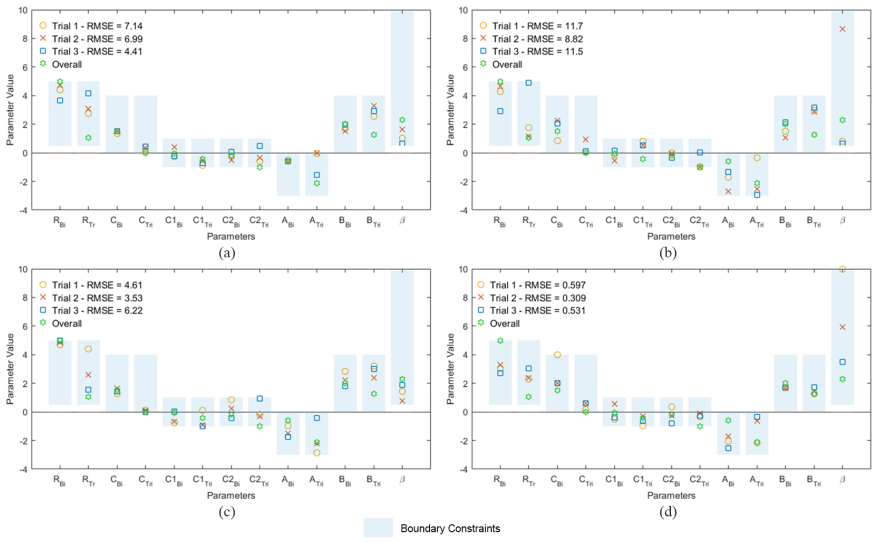

Figure 4: Comparison of neuromuscular characteristics within a) cyclic b) chirp c) resistive and d) isometric contraction tasks, for Subject A. An overall optimization was also performed on all task data, this is illustrated alongside the individually optimized task parameters. Shaded area illustrates boundary constraints for each characteristic.

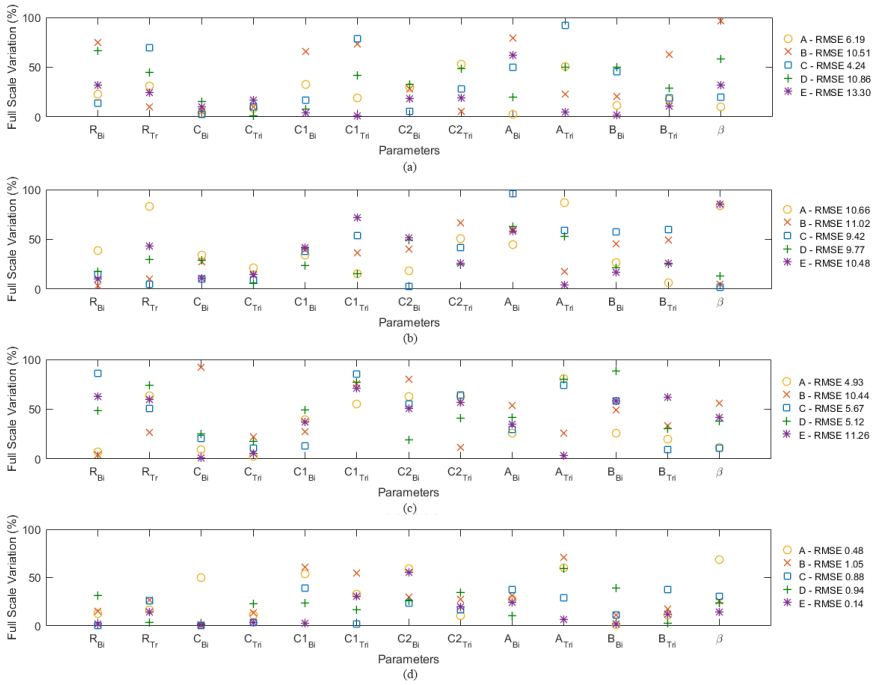

Figure 5: The full scale variation of each parameter recorded for a) cyclic b) chirp c) resistive and d) isometric contraction tasks, for each subject. The average RMS error (in degrees) across trials is also included for all tasks, for each subject. The five subjects are numbered from A to E.

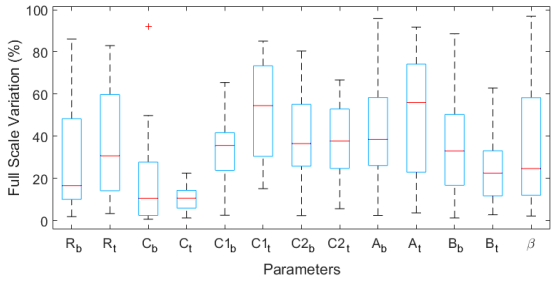

Figure 6: Box plot illustrating the variation spread, with respect to the full scale range, of each subject-specific neuromuscular characteristic across all five subjects for all recorded trials.

Table 2: Summary of Kinematic Predictions (Average RMSE)

		Predicted Kinematics			
Subject	Optimized Model	Cyclic	Chirp	Resistive	Isometric Contraction
A	*Cyclic*	16.4	27.1	110.6	17.1
	Chirp	17.6	15.4	17.4	29.4*
	Resistive	15.9	17.7	12.8	22.5
	Isometric Contraction	48.4	42.7	110.9	2.4
	Overall	**13.4**	16.4	15.1	12.4
B	*Cyclic*	23.2	15.8	37.1	84.5
	Chirp	41.7*	15.2	23.4	11.7
	Resistive	-	26.1	17.7	-
	Isometric Contraction	38.1	29.6	60.5	4.1
	Overall	26.0	18.5	21.0	6.9
C	*Cyclic*	8.7	27.6	42.4	17.2
	Chirp	19.5	14.6	25.6	-
	Resistive	80.0	56.8	31.9	-
	Isometric Contraction	22.9	28.7	48.2	1.8
	Overall	18.1	18.2	**30.1**	8.3
D	*Cyclic*	24.8	29.3	24.8*	22.9*
	Chirp	34.1*	20.1	81.6	13.5*
	Resistive	45.2*	31.4	22.5*	28.7*
	Isometric Contraction	32.9	20.8	67.8	4.5
	Overall	32.5	22.0	**20.8**	9.7
E	*Cyclic*	18.1	26.8	42.7	19.1
	Chirp	27.5	14.0	26.5	17.3
	Resistive	26.0	14.3	22.4	18.0
	Isometric Contraction	33.5	23.6	29.8	5.0
	Overall	27.6	18.6	27.7	5.5

Values reported in degrees

* = one or more trials for the task could not be predicted

- = the task could not be predicted

bold = Overall optimization lower than within-task optimization